Macromolecular Materials and Engineering
www.mme-journal.de

Flexible Sandwich Structural Strain Sensor Based on Silver Nanowires Decorated with Self-Healing Substrate

Dawei Jiang, Ying Wang, Bin Li, Caiying Sun, Zijian Wu,* Hui Yan, Lixin Xing, Shuolin Qi, Yingchun Li, Hu Liu, Wei Xie, Xiaojing Wang, Tao Ding,* and Zhanhu Guo**

Flexible and stretchable conducting composites that can sense stress or strain are needed for several emerging fields including human motion detection and personalized health monitoring. Silver nanowires (AgNWs) have already been used as conductive networks. However, once a traditional polymer is broken, the conductive network is subsequently destroyed. Integrating high pressure sensitivity and repeatable self-healing capability into flexible strain sensors represents new advances for high performance strain sensing. Herein, superflexible 3D architectures are fabricated by sandwiching a layer of AgNWs decorated self-healing polymer between two layers of polydimethylsiloxane, which exhibit good stability, self-healability, and stretchability. For better mechanical properties, the self-healing polymer is reinforced with carbon fibers (CFs). The sensors based on self-healing polymer and AgNWs conductive network show high conductivity and excellent ability to repair both mechanical and electrical damage. They can detect different human motions accurately such as bending and recovering of the forearm and shank, the changes of palm, fist, and fingers. The fracture tensile stress of the reinforced self-healing polymer (9 wt% CFs) is increased to 10.3 MPa with the elongation at break of 8%. The stretch/release responses under static and dynamic loads of the sensor have a high sensitivity, large sensing range, excellent reliability, and remarkable stability.

Dr. D. Jiang, Y. Wang, Prof. B. Li, Prof. C. Sun, S. Qi
College of Science
Northeast Forestry University
Harbin 150040, P. R. China
E-mail: libinzh62@163.com
Prof. B. Li
Post-Doctoral Mobile Research Station of Forestry Engineering
Northeast Forestry University
Harbin 150040, P. R. China
Dr. Z. Wu
Key Laboratory of Engineering Dielectrics and Its Application
Ministry of Education
Harbin University of Science and Technology
Harbin 150040, P. R. China
E-mail: zijian.wu@hrbust.edu.cn
Prof. H. Yan
School of Mechatronics Engineering
Harbin Institute of Technology
Harbin 150001, P. R. China
Dr. L. Xing
MIIT Key Laboratory of Critical Materials Technology for New Energy Conversion and Storage
School of Chemistry and Chemical Engineering
Harbin Institute of Technology
Harbin 150001, P. R. China
Prof. Y. Li
College of Materials Science and Engineering
North University of China
Taiyuan 030051, P. R. China
The ORCID identification number(s) for the author(s) of this article can be found under https://doi.org/10.1002/mame.201900074.
Prof. H. Liu, Prof. W. Xie, Prof. X. Wang, Prof. T. Ding, Prof. Z. Guo
Integrated Composites Laboratory
Department of Chemical Engineering
University of Tennessee
Knoxville 37996, USA
E-mail: dingtao@henu.edu.cn; zguo10@utk.edu
Prof. H. Liu
Key Laboratory of Materials Processing and Mold
Ministry of Education
National Engineering Research Center for Advanced Polymer Processing Technology
Zhengzhou University
Zhengzhou 450002, P. R. China
Prof. W. Xie
Key Laboratory of Lightweight and Reliability Technology for Engineering Vehicle
Education Department
Changsha University of Science and Technology
Changsha 410114, P. R. China
Prof. X. Wang
School of Material Science and Engineering
Jiangsu University of Science and Technology
Zhenjiang 212003, P. R. China
Prof. T. Ding
College of Chemistry and Chemical Engineering
Henan University
Kaifeng 475004, China

DOI: 10.1002/mame.201900074

1. Introduction

Among the reported intelligent sensors,[1,2] strain sensors have been widely used in many areas due to their response to mechanical deformations by the change of electrical characteristics such as resistance or capacitance.[3–5] However, traditional strain sensors made with metals, alloys, or piezoresistors have poor stretchability and flexiblility which limit their application areas as flexible electronics.[6,7] Nowadays, more considerable attention is focused on flexible strain sensors due to their diverse applications in electronic skin,[8–11] wearable electronics,[12,13] soft robotics,[14,15] smart textiles,[16] and structural health monitoring,[17–21] etc. A variety of carbonaceous nanomaterials or even metals were used to compound with flexible matrix as conductive fillers, such as carbon black (CB), carbon nanotube (CNT), and graphene, etc.[14–20] However, these carbonaceous composites have some obvious limitations including poor stretchability and low conductivity as compared with metals. To this end, the performance of flexible strain sensors has been improved by using flexible substrate material and thin layer of nanoconductive metals to meet the strain. In recent years, silver nanowires (AgNWs) have been used in flexible electronics due to desirable electrical and excellent mechanical properties.[21–25] For example, Amjadi et al.[26] produced a stretchable sensor consisted of AgNWs network and polydimethylsiloxane (PDMS) elastomer in the form of sandwich structure. The strain sensors based on the AgNWs network and elastomer show strong piezoresistivity and high stretchability for the motion detection of fingers and control of an avatar in the virtual environment. Lu et al.[21] fabricated strain sensors via attaching the AgNWs onto thermoplastic polyurethane electrospun membrane (TPUEM) followed by spin-coating using liquid PDMS. The strain sensor exhibited excellent conductivity, high sensitivity, excellent reliability, and remarkable stability. In particular, these efforts have been devoted to being flexible and stretchable. However, when subjected to practical applications, traditional polymer in most of these sensors will be broken, the AgNWs conductive network will then be subsequently destroyed. If the AgNWs were not interconnected, the sensors would not transmit signal any more.[27–31] Thus, an ideal flexible strain sensor should not only retain high flexibility, but also could be rapidly healed after mechanical damage.[32–35]

Self-healing polymers with the capability to repair internal cracks or external fractures by themselves have been developed over the past decades.[36–39] Once the polymer is healed, the conductive network will be healed subsequently. For example, Leibler and co-workers developed a healable thermoplastic elastomer material based on the use of dynamic hydrogen bonding for spontaneous healing.[40] This elastomer material could be easily self-healed after being broken. However, the mechanical strength of this self-healing polymer is too low to be used in any practical applications. Xing et al.[41,42] have used boron nitride nanosheets and graphene oxide to modify the polymers but the effect for strength is not ideal. Carbon fibers (CFs) have high specific strength and modulus, rigidity, excellent impact properties, and relative flexibility,[43] which have been widely used for critical components such as aerospace, marine, automobile industries, and structures such as reinforced composites by using them as fillers.[44–46] It is worth noting that the CFs with high conductivity is favorable to the improvement of both mechanical properties and piezoresistive effect. In this paper, a flexible self-healing sandwich-structured strain sensor was created with reinforced self-healing polymer/AgNWs/PDMS, where the AgNWs acted as conductive fillers, the reinforced self-healing polymer acted as self-healing substrates, and PDMS served as the encapsulating material. The reinforced self-healing polymer has been researched including self-healing and mechanical properties. The strain-sensing characteristics of the sensors including stretch/release response under static and dynamic loads, and hysteresis performance, were investigated. Meanwhile, the strain sensors were fixed to elbow joint, leg elbow, and fingers to monitor their resistance change according to different human motions. The healed sensor even demonstrated the same accurate feedback signals as the original sensor upon the human activities. From which we can infer that dynamic hydrogen bonds in the supramolecular assemblies at the fractured areas can be re-established once the damaged surfaces return into contact, thus drives the chains to diffuse and re-entangle above the glass-transition temperatures and providing self-healing.

2. Experimental Section

2.1. Materials

Empol 1016 Dimer Acid was purchased from BASF China (80% dibasic acids, 16% polybasic acids, 4% monobasic acids). The diethylenetriamine was obtained from Sigma-Aldrich. Silver nitrate ($AgNO_3$) was obtained from Sinopharm Chemical Reagent Co., Ltd. China. PDMS (Sylgard 184 Silicone Elastomer) was purchased from Dow Corning Corp., and supplied as two-part liquid component kits. Sodium chloride (NaCl) was bought from Zhiyuan Reagent Co., Ltd. Tianjin, China. Ethylene glycol (EG), methyl alcohol, and chloroform were supplied by Tianjin Tianli Fine chemical Co., Ltd. Tianjin, China. All the chemical reagents were used as received without any further purification.

2.2. Fabrication of Reinforced Self-Healing Polymer Nanocomposites

The self-healing polymer nanocomposites were prepared with the following procedures. Briefly, Empol 1016 Dimer Acid (30 g, 0.104 mol) and diethylenetriamine (12.3 g, 0.119 mol) were mixed at 160 °C for 24 h with intensive magnetic stirring and under a nitrogen atmosphere. The resultant mixture was dissolved in 150 mL chloroform and then washed with 450 mL mixed solvent of methanol and water (1:2 by volume) followed by vacuum removal of chloroform. Five gram resulting polymer and 1.18 g urea were dissolved in 5 mL ethanol and then mixed with chopped carbon fibers (stage addition) in the required ratios under sonication for 30 min at room temperature to obtain a homogeneous mixture under mechanical stirring. Then, the temperature was raised to 135 °C for 1 h and increased by 5 °C every hour till 160 °C then kept for 1.5 h, and then dried under vacuum and pressed at 100 °C in a 1 mm thick tetrafluoroethylene (Tefl) mold to form reinforced self-healed polymer composite films.

2.3. Fabrication of Silver Nanowires

AgNWs were prepared using a modified polyol method.[47] Briefly, ≈0.5 g Polyvinyl Pyrrolidone (PVP) was dissolved in 50 mL ethylene glycol (EG) by heating the solution to 170 °C by magnetically stirring for 1 h. NaCl (50 µL, 0.1 M) EG solution was heated to 170 °C and then added into the flask, and stirred for 10 min. Then, 50 mL 0.059 M $AgNO_3$ in EG was injected drop by drop into the solution at a rate of 5 mL min^{-1}. The color was glistening gray, indicating the formation of long AgNWs. The reaction was allowed to cool down to room temperature after 24 h. The solution was then centrifuged (five times at 5000 rpm) to remove EG, PVP, and other impurities from supernatant after adding acetone. The AgNWs were suspended in ethanol at a concentration of 0.2 mg mL^{-1} (Figure S1, Supporting Information). The length and diameter of the AgNWs were ≈20 µm and ≈100 nm, respectively (Figure S1, Supporting Information).

2.4. Fabrication of Self-Healing Sandwich-Structured Strain Sensors

The strain sensors were fabricated according to the following procedures. Briefly, 2 mL AgNWs solution was first dropcast onto the middle part of tetrafluoroethylene plate, which was then put in the oven at 60 °C for 1 h. Subsequently, one piece of reinforced self-healed polymer composites was covered on the plate, which was heated at 90 °C for 30 s and then hot pressed at 0.2 MPa for 1 min. The sample of AgNWs decorated self-healing polymer was obtained after cooling it down to room temperature. This sample was cut into two same pieces with a length of 40 mm and a width of 10 mm. Two copper conductors were adhered to both ends of one slice (the side containing AgNWs) with conductive silver adhesives, and then were covered with the other slice (the side containing AgNWs) to make sandwich structure of self-healing polymer composites with AgNWs. The mixture of liquid PDMS and curing agent (10:1) was casted onto a standard glass slide at 60 °C for 15 min. Then the sandwich structure of self-healing polymer composites was placed on the surface of PDMS followed by continuously casting the same content of the mixture of liquid PDMS and curing agent at 60 °C for 30 min to form the self-healing sandwich-structured strain sensors.

2.5. Characterization

The morphologies of the samples were characterized by scanning electron microscopy (SEM, Hitachi, SU8020). The stretching and bending experiments of the strain sensors were all carried out using an electronic universal tensile testing machine (WDW-2, Jinan Yongke Testing Instrument Co., Ltd.). The electrical resistances of the specimens were measured in situ by a digit precision multimeter (Agilent, 34401A).

3. Results and Discussion

Figure 1 and Figure S2, Supporting Information, shows the schematic illustration of reinforced self-healing polymer composite preparation and self-healing mechanism. The supramolecular network was formed through the polycondensation between diethylene triamine and fatty acids according to the reference.[40] Subsequently, the chopped carbon fibers (as received) and urea were added into the supramolecular network to prepare the reinforced self-healing polymer composite system. In this system, the self-healing resulted from the hydrogen-bond interaction between N–H bond and C=O bond while the chopped carbon fibers acted as reinforcement.[41,48]

The hydrogen-bond interaction has been demonstrated to dynamically dissociate and associate at certain conditions (e.g., certain temperature or pressure), however, the interaction is very weak so as to cause a poor mechanical performance which hardly allows them to be applied for real applications.[49] Carbon fibers are traditional micron reinforcing materials with high strength, high stiffness, and light weight,[50] and thus can offer high specific modulus and high specific strength. The mechanical strength of the reinforced self-healing polymer composite has a dramatic improvement followed by the introduction of carbon

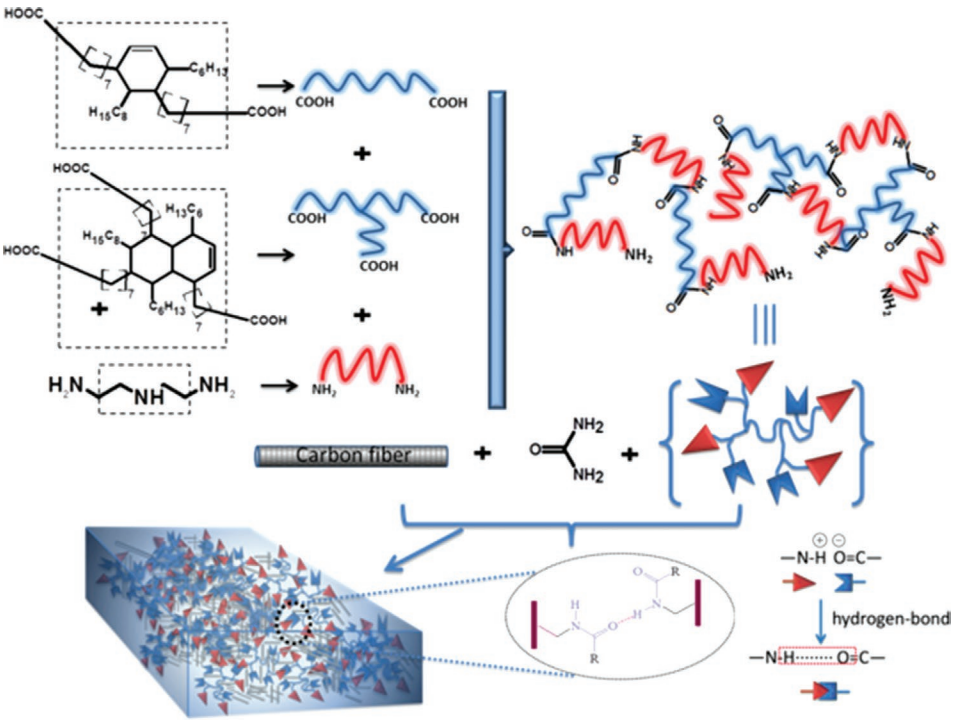

Figure 1. Schematic illustration of the synthesis of reinforced self-healed polymer composite.

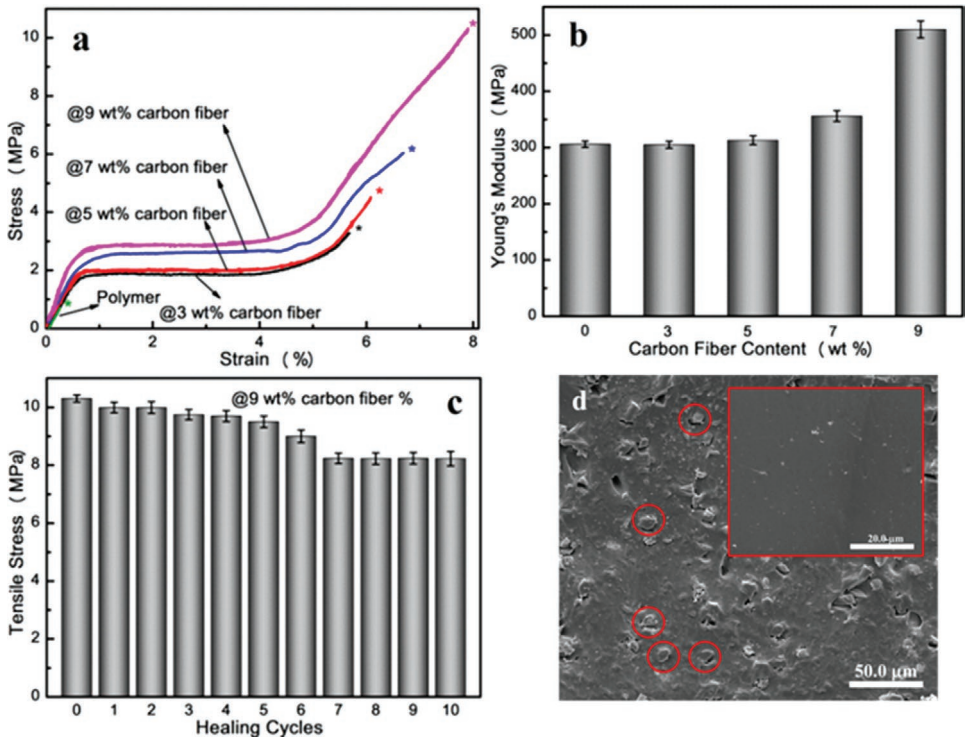

Figure 2. a,b) The tensile strain–stress curves and Young's modulus of reinforced self-healed polymer composites with different carbon fiber contents, c) the tensile strength of 9 wt% carbon fiber sample versus healing cycles, d) Cross-sectional SEM image of the reinforced self-healed polymer composites with 9 wt% carbon fiber. Inset: Cross-sectional SEM image of pure polymer.

fibers compared with pure supramolecular polymeric network (**Figure 2**a,b). The tensile strength and Young's modulus have been increased with increasing the carbon fiber content. The maximum tensile strength and Young's modulus are 10.3 and 510 MPa (9 wt% carbon fiber), respectively, compared with pure polymer without carbon fiber (just 0.7 and 306 MPa). The elongation at break of reinforced self-healing polymer composites with 9 wt% carbon fibers (near 8%) is nearly 27 orders of magnitude increase compared with that of pure polymer network. (just near 0.3%). Notably, pure polymer could not be directly used as material due to their intrinsic weak and brittle nature. However the polymer becomes stronger and tougher after the incorporation of carbon fibers into the supramolecular polymeric network. From Figure S3, Supporting Information, the reinforced self-healing polymer composites with 9 wt% carbon fibers show a glass transition temperature of 32 °C, which is lower than that of pure polymer of 35 °C. The lower glass transition temperature is more beneficial for self-healing of polymer composites.

The tensile strength of reinforced self-healing polymer composite has hardly been decreased in the first five healing cycles (Figure 2c) and has a 20% decline after six healing cycles, which remains unchanged till ten healing cycles. All of these healing cycles are in the case of 60 °C for 3 h. If the test is extended to 24 h, the tensile strength of reinforced self-healing polymer composites would be 100% self-repaired even in ten healing cycles (Table S1, Supporting Information). As shown in Figure 2d, the morphology of the cross section reinforced self-healing polymer composites with 9 wt% carbon fibers revealed that the carbon fibers are well dispersed in the polymer matrix even when the fibers content reaches up to 9 wt%. The SEM image of cross section for pure polymer shows that the surface is very smooth without any protrusions or depressions. Compared to pure polymer, the cross section of the reinforced self-healing polymer composites with 9 wt% carbon fibers shows distinct carbon fibers cross-sectional shape and are uniformly distributed in the polymer matrix. The distributed carbon fibers are marked with red circles (Figure 2d). No aggregate of carbon fibers is observed in the supramolecular polymeric network otherwise it will seriously influence the self-repairing action of reinforced self-healed polymer composites.

Self-healing effect has not been significantly decreased with increasing the carbon fiber content. On the contrary, the mechanical property is promoted with increasing the carbon fiber content. **Figure 3** shows the photos and optical microscopy images of the process of cutting and healing. Self-healing condition has remained nearly the same during each cycle of cutting and healing, indicating no aging of reinforced self-healing polymer composites with mechanical breakdown. It shows that the self-healing polymer has a stable repairing performance and does not decay with increasing the number of reparation. The surface of reinforced self-healed polymer composites has a very small crack at the seventh healing cycle, nevertheless the crack has not been observed during the first six healing cycles. The crack accounts for the compromised mechanical properties of reinforced self-healing polymer composite. Even though there would be a small crack on the surface of reinforced self-healed polymer composites, the usability of composite is not affected.

Figure 4a presents the process for manufacturing integrated self-healing sandwich-structured strain sensors (detailed

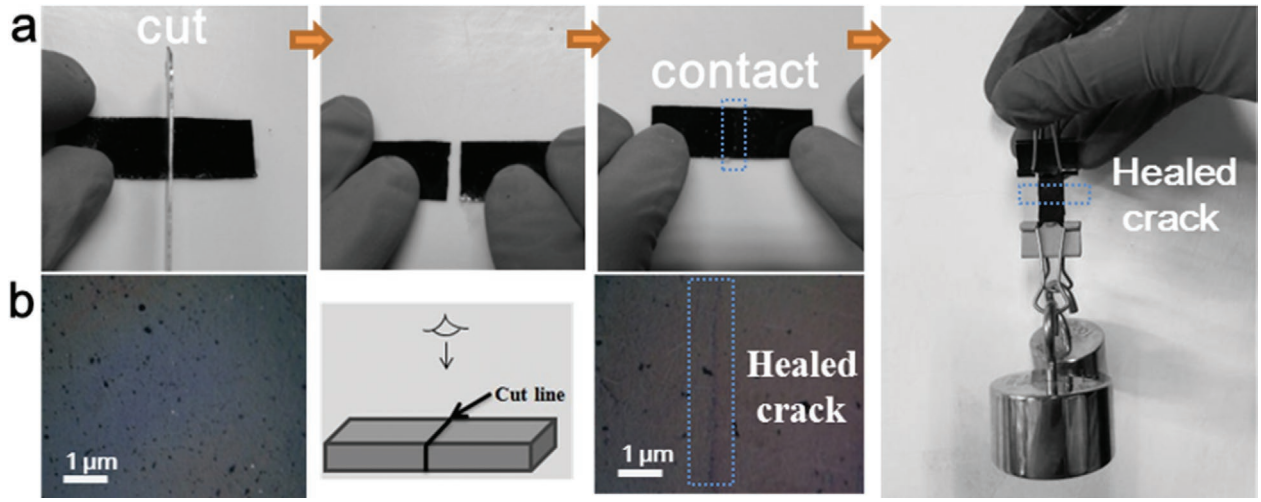

Figure 3. a) Photographs portraying the self-reparability of reinforced self-healed polymer composites with 9 wt% carbon fiber content along the direction of the arrow. b) Optical microscopy images of the surface of reinforced self-healed polymer composites (9 wt% carbon fiber content) without damage (left) and healed at 60 °C for 3 h after damage (right).

preparation processes are described in the Experimental Section). Figure 4b shows that the sandwich-structured strain sensors can be twisted and bended with excellent stretchability, flexibility, and bendability. The adhesive tape is made into a regular shape and adhered on a Tefl plate so that the silver nanowire solution is evenly distributed on the surface, and the solidified silver nanowire layer can be obtained after drying at 60 °C. The reinforced self-healing polymer composites served as self-healing substrates and the AgNWs film with a thickness of 0.1 mm was cast in the middle of two pieces of self-healing substrates as conductive network. Inserting a layer of AgNWs network between two layers of self-healing polymer guarantees both high piezoresistive sensitivity and excellent self-healability. Then the composite is embedded between two layers of PDMS forming integrated self-healing sandwich-structured strain sensors.

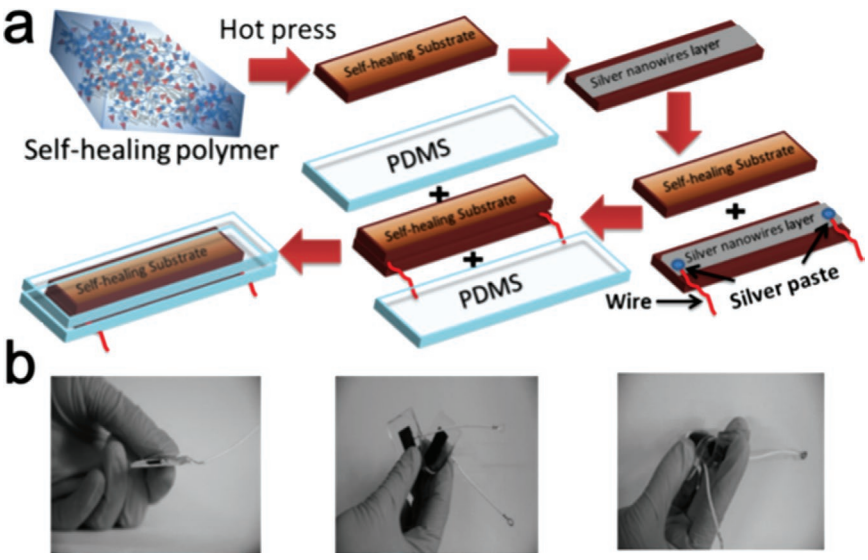

Figure 4. a) Schematic illustration of fabricating sandwich-structured strain sensors, b) photographs of the strain sensor under bending and twisting.

The AgNWs are well dispersed in the surface of reinforced self-healing polymer composites with 9 wt% carbon fibers (**Figure 5**a). While the reinforced self-healing polymer composites with 9 wt% carbon fibers were made into sandwich structure, the AgNWs layers were evenly distributed at the interface of two pieces of reinforced self-healing polymer composites with 9 wt% carbon fibers (Figure 5b).

The resistance of self-healing sandwich-structured strain sensor is just 3.114 Ω for lighting the light-emitting diodes (LEDs) shown in **Figure 6**. The conductivity of the sensor caused by well-developed electric conductivity of AgNWs indicates the dispersion and density loading of AgNWs at the interface of two pieces of self-healing substrates. While the integrated self-healing conductive composites in the sandwich-structured strain sensor were broken, the electrical conductivity of the sensor disappeared, the resistance became infinite and thus the LEDs could not be lighted. Interestingly, the resistance of the sensor recovers to the level similar to the pristine value, and the LEDs (3.412 Ω) are lighted again. This phenomenon illustrates that 3D AgNWs network has been broken following the breakage of self-healing conductive composite. 3D AgNWs network has been established again after the self-healing of the composites (Figure S4, Supporting Information). The repairing process has not influenced the AgNWs network.

The responses of the sandwich-structured strain sensor to the dynamic loading profile and hysteresis curve are shown in **Figure 7** and Figure S5, Supporting Information, respectively. The response of sandwich-structured strain sensor for the stretch/release cycles is in good agreement with the loading profile, there is no obvious drifting and hysteresis in the

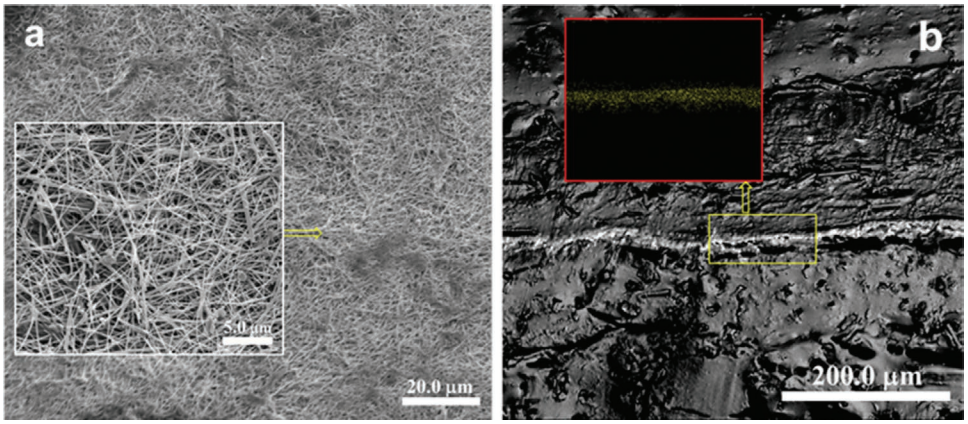

Figure 5. a) Superficial SEM image of reinforced self-healed polymer composites with 9 wt% carbon fibers with AgNWs, b) Cross-sectional backscatter electron image of sandwich structure of self-healed polymer composite with AgNWs. Inset: Argentum element mapping on the cross section of the sandwich structure of self-healed polymer composite with AgNWs established using energy dispersion spectrum (EDS).

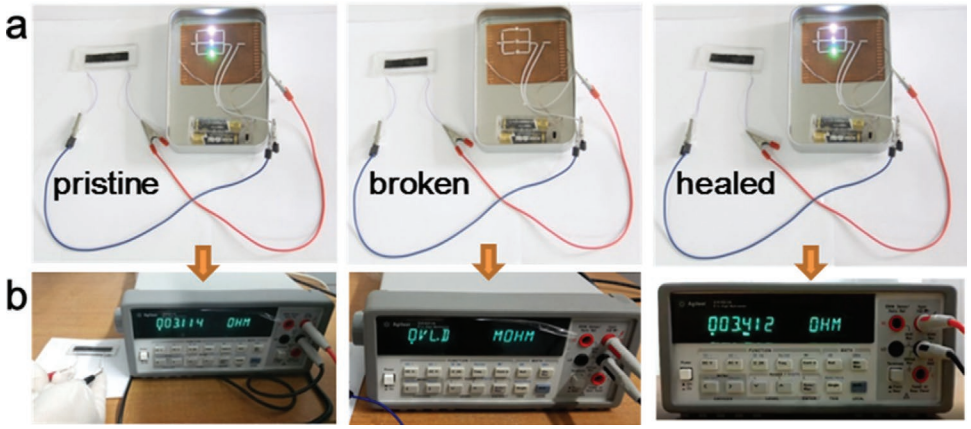

Figure 6. a) Photographs showing the lighting of white light emitting diode (LED) bulb, b) resistance of pristine, broken, and healed strain sensors.

response of the strain sensors even for ε larger than 40% of the stretch/release cycles, indicating a better performance compared with CNT based strain sensors just $\varepsilon = 20\%$.[51–53] Even the sandwich-structured strain sensor with a larger strain (e.g., $\varepsilon = 60\%$) shows a smaller hysteresis in the response compared with the sandwiched structured strain sensors of just AgNWs-PDMS nanocomposites in the reference.[26]

Due to good flexibility, high stretchability, and excellent stability of the self-healing sandwich-structured strain sensor, a variety of applications was then conducted for monitoring the human motions. The sensor to detect the rapid bending and recovering of the forearm and shank was carried out by fixing the sensor onto the elbow joint and leg elbow (**Figure 8**a,b). The movement curve of the forearm shows an accurate response.

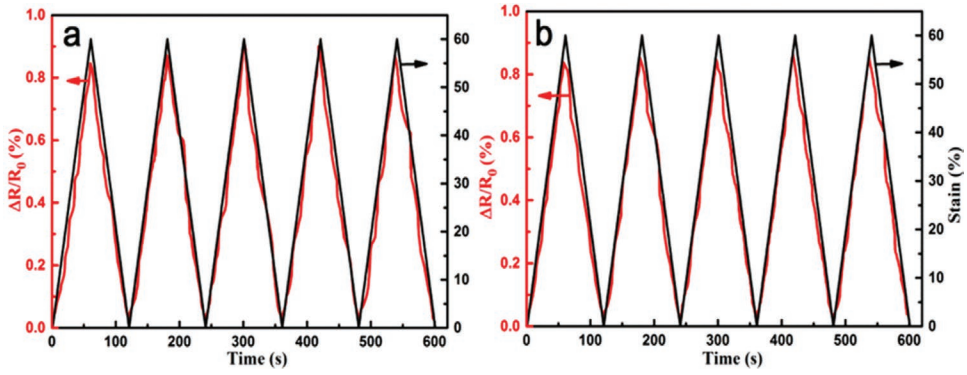

Figure 7. Response of the sandwich-structured strain sensor under stretch/release cycles of $\varepsilon = 60\%$, a) pristine, b) healed strain sensor.

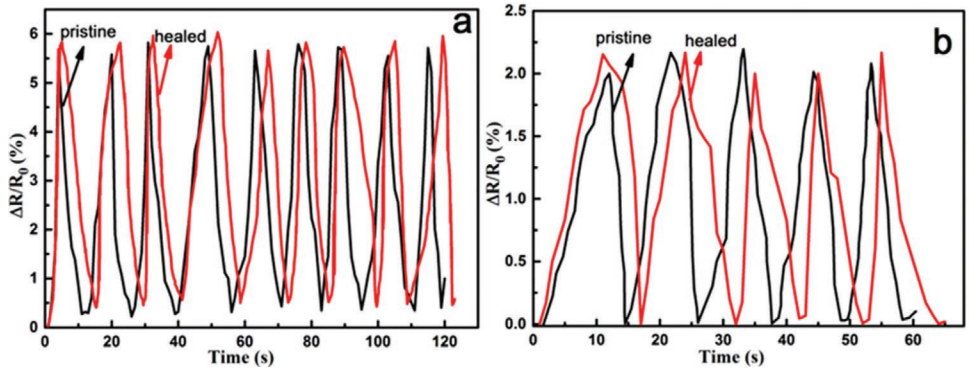

Figure 8. Responses of sandwich-structured strain sensors to cyclic motions of a) forearm bending and recovering, b) shank bending and recovering.

Nine periodic actions of bending and recovering of the forearm have been taken for the forearm, and nine periodic regular peaks are recorded. The curve is very stable and the resistance change is nearly the same for each period. This tendency could also be observed in the healed sensor, indicating that the reparation process has not influenced the response of the sensor to human motions. The response of the sensors to the rapid bending and recovering of the shank is a little big compared with the arm and fingers (Figure 8b). This is owing to the fact that the leg movements are not flexible as the arm, and the leg joint is thicker than the elbow. This is also confirmed from the resistance change of sensor to be applied to the legs which is lower than that of the forearm movement.

It can be concluded that the self-healing sandwich-structured strain sensor in this paper can be used in monitoring various human motions whether original or healed. Various human motions could give different resistance changes. Once one certain part of human body changes, the response of the sensor will vary accompanied with daily activities. The "gauge factor" (GF, GF = $(\Delta R/R_0)/\varepsilon$, where ε is strain value, ΔR is the resistance change between the resistance at a strain, and R_0 is the initial resistance) represents the strain sensor sensitivity. The higher the GF value of a sensor, the more sensitive it is. However, high GFs mean excessive sensitivity which can result in excessive signal amplitude and thus needs a wider sensing system dynamic range. Thus, both appropriate strain variation sensitivity and consistent electric circuit sensing system are required. The GF of our sandwich-structured strain sensor is 1.5 but it can detect the human motions accurately. In this case, the motions of palm, fist, and finger have been detected (**Figure 9**). For the motion of a palm, there is no signal changing, however the resistance change starts to rise as soon as the palm begins to bend. While the palm completely turned into fist, the resistance change rate reaches the maximum. If we keep this motion, the resistance has no change. Then the motion recovers from fist to palm, the resistance is recovered. As the thumb, the ring finger and the little finger bending at the same time, the resistance is increased again. The larger the bending degree, the bigger the resistance increase can be observed.

However, the maximum is lower than that of the fists since the index finger and middle finger are not bended. The healed sensor has nearly the same result indicating that the repairing process has not influenced the detection of human motion. These motions have the same tendency, exhibiting a good stability, response speed.

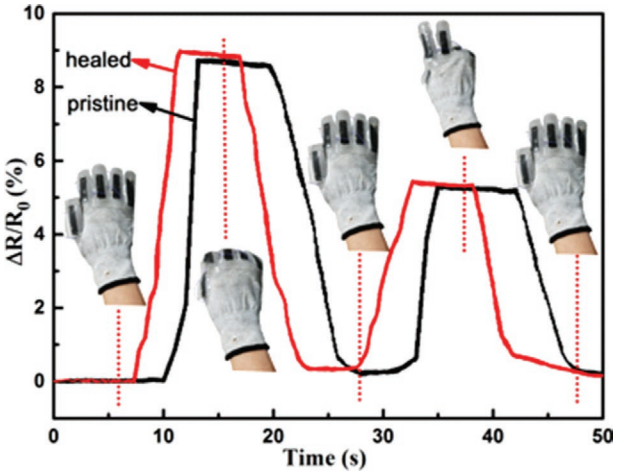

Figure 9. Responses of sandwich-structured strain sensors to cyclic motions with different finger bending and recovering.

4. Conclusion

Self-healing sandwich-structured strain sensors have been developed with high sensitivity, stretchability, and stability with low cost and simple fabrication process based on the sandwich-structured reinforced self-healing polymer/AgNWs/PDMS. The reinforced self-healing polymer has been successfully fabricated with high mechanical strength. The fracture tensile stress of reinforced self-healing polymer (9% carbon fiber) has increased to 10.3 MPa with the elongation at break of 8% compared with that of pure polymer just 1.0 MPa with the elongation at break of 0.3%. The stretch/release response under static and dynamic loads of the sensor has high sensitivity, large sensing range (ε = 60%), excellent reliability, and remarkable stability. Different human motions were monitored through sensor, raveling that different human movements give different accompanied signals for the self-healing properties of the sensor including conductivity and sensing performance, which increase the lifetime of the sensor. This study provides a foundation for practical applications of the self-healed flexible sensor due to

the self-healing properties, excellent reliability, and remarkable stability. The sensing performance of our sensor before and after self-healing has been successfully demonstrated by the detection of different human movements, which indicates that a combination of high pressure sensitivity and repeatable self-healing capability can be achieved simultaneously.

Supporting Information

Supporting Information is available from the Wiley Online Library or from the author.

Acknowledgements

This work was supported by Fundamental Research Funds for the Central Universities (No. 2572018BC27), China Postdoctoral Science Foundation (No. 2016M601402 & 2017M610212), Heilongjiang Postdoctoral Foundation (No. LBH-Z16004, LBH-Z16089), and Heilongjiang Postdoctoral Special Foundation (No. LBH-TZ1713). Key Laboratory of Engineering Dielectrics and Its Application (HUST)- Ministry of Education, Heilongjiang Natural Science Foundation (QC2017038).

Conflict of Interest

The authors declare no conflict of interest.

Keywords

flexibility, polydimethylsiloxane, self-healing, sensors, silver nanowires

Received: January 29, 2019
Revised: March 24, 2019
Published online: April 25, 2019

[1] a) H. Gu, H. Zhang, J. Lin, Q. Shao, D. P. Young, L. Sun, T. D. Shen, Z. Guo, *Polymer* **2018**, *143*, 324; b) X. Xiang, F. Pan, Y. Li, *Eng. Sci.* **2018**, *3*, 77; c) J. Cai, W. Xu, Y. Liu, Z. Zhu, G. Liu, W. Ding, G. Wang, H. Wang, Y. Luo, *Eng. Sci.* **2019**, *5*, 21; d) H. Gu, H. Zhang, C. Gao, C. Liang, J. Gu, Z. Guo, *ES Mater. Manuf.* **2018**, *1*, 3; e) M. Chen, J. Zhu, B. Yang, X. Yao, X. Zhu, Q. Liu, X. Lyu, *Adv. Compos. Hybrid Mater.* **2018**, *1*, 612.

[2] a) L. Gao, L. Zhang, X. Lyu, G. Lu, Q. Liu, *Eng. Sci.* **2019**, *1*, 69; b) S. Kudaibergenov, J. Koetz, N. Nuraje, *Adv. Compos. Hybrid Mater.* **2018**, *1*, 649; c) R. Zhou, Z. Lin, L. Xin, J. Song, H. Liu, Z. Guo, *Adv. Compos. Hybrid Mater.* **2018**, *1*, 785.

[3] a) Y. Lu, M. C. Biswas, Z. Guo, J. Jeon, E. K.Wujcik, *Biosens. Bioelectron.* **2019**, *123*, 167; b) X. Liu, C. Lu, X. Wu, X. Zhang, *J. Mater. Chem. A* **2017**, *5*, 9824; c) Y. Li, B. Zhou, G. Zheng, X. Liu, T. Li, C. Yan, C. Cheng, K. Dai, C. Liu, C. Shen, Z. Guo, *J. Mater. Chem. C* **2018**, *6*, 2258; d) S. Zhang, H. Liu, S. Yang, X. Shi, D. Zhang, C. Shan, L. Mi, C. Liu, C. Shen, Z. Guo, *ACS Appl. Mater. Interfaces* **2019**, *11*, 10922; e) H. Liu, M. Dong, W. Huang, J. Gao, K. Dai, J. Guo, G. Zheng, C. Liu, C. Shen, Z. Guo, *J. Mater. Chem. C* **2017**, *5*, 73.

[4] a) T. Lee, W. C. Yong, G. Lee, P. V. Pikhitsa, D. Kang, M. K. Sang, M. Choi, *J. Mater. Chem. C* **2016**, *4*, 9947; b) H. Gu, H. Zhang, C. Ma, H. Sun, C. Liu, K. Dai, J. Zhang, R. Wei, T. Ding, Z. Guo, *J. Mater. Chem. C* **2019**, *7*, 2353; c) H. Liu, Q. Li, S. Zhang, R. Yin, X. Liu, Y. He, K. Dai, C. Shan, J. Guo, C. Liu, C. Shen, X. Wang, N. Wang, Z. Wang, R. Wei, Z. Guo, *J. Mater. Chem. C* **2018**, *6*, 12121; d) X. Ye, Z. Yuan, H. Tai, W. Li, X. Du, Y. Jiang, *J. Mater. Chem. C* **2017**, *5*, 7746; e) C. Koomson, S. Zeltmann, N. Gupta, *Adv. Compos. Hybrid Mater.* **2018**, *2*, 341.

[5] a) Q. Zhang, Q. Liang, Q. Liao, M. Ma, F. Gao, X. Zhao, Y. Song, L. Song, X. Xun, Y. Zhang, *Adv. Funct. Mater* **2018**, *28*, 1803117; b) Q. Zhang, Q. Liang, Q. Liao, F. Yi, X. Zheng, M. Ma, F. Gao, Y. Zhang, *Adv. Mater.* **2017**, *29*, 1606703.

[6] S. H. Shin, D. H. Park, J. Y. Jung, H. L. Min, J. Nah, *ACS Appl. Mater. Interfaces* **2017**, *9*, 9233.

[7] D. Kwon, T. I. Lee, J. Shim, S. Ryu, M. S. Kim, S. Kim, T. S. Kim, I. Park, *ACS Appl. Mater. Interfaces* **2016**, *8*, 16922.

[8] Y. Li, B. Zhou, G. Zheng, X. Liu, T. Li, C. Yan, C. Cheng, K. Dai, C. Liu, C. Shen, *J. Mater. Chem. C* **2017**, *6*, 2258.

[9] M. Wang, K. Zhang, X. X. Dai, Y. Li, J. Guo, H. Liu, G. H. Li, Y. J. Tan, J. B. Zeng, Z. Guo, *Nanoscale* **2017**, *9*, 11017.

[10] X. Li, T. Yang, Y. Yang, J. Zhu, L. Li, F. E. Alam, X. Li, K. Wang, H. Cheng, C. T. Lin, *Adv. Funct. Mater* **2016**, *26*, 1322.

[11] G. Yu, J. Hu, J. Tan, Y. Gao, Y. Lu, F. Z. Xuan, *Nanotechnology* **2018**, *29*, 115502.

[12] X. Fang, J. Tan, Y. Gao, Y. Lu, F. Xuan, *Nanoscale* **2017**, *9*, 17948.

[13] H. Liu, J. Gao, W. Huang, K. Dai, G. Zheng, C. Liu, C. Shen, X. Yan, J. Guo, Z. Guo, *Nanoscale* **2016**, *8*, 12977.

[14] a) J. C. Yeo, H. K. Yap, W. Xi, Z. Wang, C. H. Yeow, C. T. Lim, *Adv. Funct. Technol.* **2016**, *1*, 1600018; b) H. Liu, Y. Li, K. Dai, G. Zheng, C. Liu, C. Shen, X. Yan, J. Guo, Z. Guo, *J. Mater. Chem. C* **2016**, *4*, 157; c) Y. He, Q. Chen, S. Yang, C. Lu, M. Feng, Y. Jiang, G. Cao, J. Zhang, C. Liu, *Compos. A* **2018**, *108*, 12; d) X. Li, S. Zhao, W. Hu, X. Zhang, L. Pei, Z. Wang, *Appl. Surface Sci.* **2019**, *481*, 374; e) L. Ma, N. Li, G. Wu, G. Song, X. Li, P. Han, G. Wang, Y. Huang. *Appl. Surf. Sci.* **2018**, *433*, 560; f) H. Gu, X. Xu, M. Dong, P. Xie, Q. Shao, R. Fan, C. Liu, S. Wu, R. Wei, Z. Guo, *Carbon* **2019**, *147*, 550.

[15] a) C. Hu, Z. Li, J. Gao, K. Dai, G. Zheng, C. Liu, C. Shen, H. Song, Z. Guo, *J. Mater. Chem. C* **2017**, *5*, 2318; b) S. Din, W. Xu, L. K. Cheng, S. Dirven, *IEEE Sens. J.* **2017**, *17*, 5678; c) L. Ma, Y. Zhu, M. Wang, X. Yang, G. Song, Y. Huang. *Compos. Sci. Technol.* **2019**, *170*, 148; d) G. Zhu, X. Cui, Y. Zhang, M. Dong, H. Liu, Q. Shao, T. Ding, S. Wu, Z. Guo, *Polymer* **2019**, in press; e) J. Zhang, P. Li, Z. Zhang, X. Wang, J. Tang, H. Liu, Q. Shao, T. Ding, A. Umar, Z. Guo, *J. Colloid Interface Sci.* **2019**, *542*, 159.

[16] a) T. Lee, W. Lee, S. W. Kim, J. J. Kim, B. S. Kim, *Adv. Funct. Mater* **2016**, *26*, 6206; b) R. Ma, Y. Wang, H. Qi, C. Shi, G. Wei, L. Xiao, Z. Huang, S. Liu, H. Yu, C. Teng, H. Liu, V. Murugadoss, J. Zhang, Y. Wang, Z. Guo, *Compos. B* **2019**, *167*, 396; c) S. Shi, L. Wang, Y. Pan, C. Liu, X. Liu, Y. Li, J. Zhang, G. Zheng, Z. Guo, *Compos. B* **2019**, *167*, 362; d) Q. Chen, Q. Yin, A. Dong, Y. Gao, Y. Qian, D. Wang, M. Dong, Q. Shao, H. Liu, B. Han, T. Ding, Z. Guo, N. Wang, *Polymer* **2019**, *169*, 255; e) X. Gong, Y. Liu, Y. Wang, Z. Xie, Q. Dong, M. Dong, H. Liu, Q. Shao, N. Lu, V. Murugadoss, T. Ding, Z. Guo, *Polymer* **2019**, *168*, 131; f) W. Xie, Z. Chen, H. Cheng, Z. Chu, J. Kuang, *New Carbon Mater.* **2011**, *26*, 441.

[17] a) J. D. Pegan, J. Zhang, M. Chu, T. Nguyen, S. J. Park, A. Paul, J. Kim, M. Bachman, M. Khine, *Nanoscale* **2016**, *8*, 17295; b) C. Hou, Z. Tai, L. Zhao, Y. Zhai, Y. Hou, Y. Fan, F. Dang, J. Wang, H. Liu, *J. Mater. Chem. A* **2018**, *6*, 9723; c) Z. Zhao, P. Bai, L. Li, J. Li, L. Wu, P. Huo, L. Tan, *Materials* **2019**, *12*, 330; d) Z. Zhao, J. Li, P. Bai, H. Qu, M. Liang, H. Liao, L. Wu, P. Huo, H. Liu, J. Zhang, *Metals* **2019**, *9*, 267; e) Y. Zhao, B. Zhang, H. Hou, W. Chen, M. Wang, *J. Mater. Sci. Technol.* **2019**, *35*, 1044; f) M. Liu, B. Li, H. Zhou, C. Chen, Y. Liu, T. Liu, *Chem. Commun.* **2017**, *53*, 2810.

[18] a) M. V. Shuba, D. I. Yuko, P. P. Kuzhir, S. A. Maksimenko, M. Crescenzi, M. Scarselli, *Nanotechnology* **2018**, *29*, 375202; b) Y. Zhao, L Qi, Y Jin, K. Wang, J. Tian, P. Han, *J. Alloys Compounds*

2015, *647*, 1104; c) W. Xie, X. Zhu, S. Yi, J. Kuang, H. Cheng, W. Tang, Y. Deng. *Mater. Des.* **2016**, *90*, 38; d) M. Dong, Q. Li, H. Liu, C. Liu, E. Wujcik, Q. Shao, T. Ding, X. Mai, C. Shen, Z. Guo, *Polymer* **2018**, *158*, 381; e) Z. Wu, S. Gao, L. Chen, D. Jiang, Q. Shao, B. Zhang, Z. Zhai, C. Wang, M. Zhao, Y. Ma, X. Zhang, L. Weng, M. Zhang, Z. Guo, *Macromol. Chem. Phys.* **2017**, *218*, 1700357.

[19] a) S. Drieschner, M. V. Seckendorff, E. D. Corro, J. Wohlketzetter, B. M. Blaschke, M. Stutzmann, J. A. Garrido, *Nanotechnology* **2018**, *29*, 225402; b) Y. Zhao, X. Tian, B. Zhao, Y. Sun, H. Guo, M. Dong, H. Liu, X. Wang, Z. Guo, A. Umar, H. Hou, *Sci. Adv. Mater.* **2018**, *10*, 1793; c) W. Xie, H. Cheng, Z. Chu, Z. Chen, C. Long, *Ceram. Int.* **2011**, *37*, 1947; d) Z. Wu, H. Cui, L. Chen, D. Jiang, L. Weng, Y. Ma, X. Li, X. Zhang, H. Liu, N. Wang, J. Zhang, Y. Ma, M. Zhang, Y. Huang, Z. Guo, *Compos. Sci. Technol.* **2018**, *164*, 195; e) H. Du, C. Zhao, J. Lin, Z. Hu, Q. Shao, J. Guo, B. Wang, D. Pan, E. Wujcik, Z. Guo, *Chem. Rec.* **2018**, *18*, 1365; f) C. Wang, V. Murugadoss, J. Kong, Z. He, X. Mai, Q. Shao, Y. Chen, L. Guo, C. Liu, S. Angaiah, Z. Guo, *Carbon* **2018**, *140*, 696.

[20] a) W. Zhang, C. Y. Hou, Y. G. Li, Q. H. Zhang, H. Z. Wang, *Nanoscale* **2017**, *9*, 17821; b) W. Xie, H. Cheng, J. Kuang, Z. Chen, Z. Chu, *J. Inorganic Mater.* **2011**, *26*; 939; c) N. Wu, D. Xu, Z. Wang, F. Wang, J. Liu, W. Liu, Q. Shao, H. Liu, Q. Gao, Z. Guo, *Carbon* **2019**, *145*, 433; d) H. Gu, H. Zhang, C. Ma, X. Xu, Y. Wang, Z. Wang, R. Wei, H. Liu, C. Liu, Q. Shao, X. Mai, Z. Guo, *Carbon* **2019**, *142*, 131; e) Y. He, S. Yang, H. Liu, Q. Shao, Q. Chen, C. Lu, Y. Jiang, C. Liu, Z. Guo, *J. Colloid Interface Sci.* **2018**, *517*, 40; f) M. Dong, C. Wang, H. Liu, C. Liu, C. Shen, J. Zhang, C. Jia, T. Ding, Z. Guo, *Macromol. Mater. Eng.* **2019**, *304*, 1900010

[21] F. Yi, X. F. Wang, S. M. Niu, S. M. Li, Y. J. Yin, K. R. Dai, G. J. Zhang, L. Lin, Z. Wen, H. Y. Guo, J. Wang, M. H. Yeh, Y. L. Zi, Q. L. Liao, Z. You, Y. Zhang, Z. L. Wang, *Sci. Adv.* **2016**, *2*, 1501624.

[22] H. T. Niu, H. Zhou, H. X. Wang, T. Lin, *Macromol. Mater. Eng.* **2016**, *301*, 707.

[23] F. Wu, Z. D. Li, F. Ye, X. L. Zhao, T. Zhang, X. N. Yang, *J. Mater. Chem. C* **2016**, *4*, 11074.

[24] J. G. Lee, J. H. Lee, S. An, D. Y. Kim, T. G. Kim, S. S. Al-Deyab, A. L. Yarin, S. S. Yoon, *J. Mater. Chem. A* **2017**, *5*, 6677.

[25] B. Bari, J. Lee, T. Jang, P. Won, S. H. Ko, K. Alamgir, M. Arshad, L. J. Guo, *J. Mater. Chem. A* **2016**, *4*, 11365.

[26] M. Amjadi, A. Pichitpajongkit, S. Lee, S. Ryu, I. Park, *ACS Nano* **2014**, *8*, 5154.

[27] S. Chen, Y. Wei, S. Wei, Y. Lin, L. Liu, *ACS Appl. Mater. Interfaces* **2016**, *8*, 25563.

[28] Y. Lee, S. Y. Min, T. W. Lee, *Macromol. Mater. Eng.* **2017**, *302*, 10.

[29] D. S. Leem, A. Edwards, M. Faist, J. Nelson, D. D. Bradley, J. C. de Mello, *Adv. Mater.* **2011**, *23*, 4371.

[30] R. Zhu, C. H. Chung, K. C. Cha, W. Yang, Y. B. Zheng, H. Zhou, T. B. Song, C. C. Chen, P. S. Weiss, G. Li, *ACS Nano* **2011**, *5*, 9877.

[31] T. Akter, W. S. Kim, *ACS Appl. Mater. Interfaces* **2012**, *4*, 1855.

[32] D. J. Lipomi, M. Vosgueritchian, B. C. Tee, B. C. Tee, S. L. Hellstrom, J. A. Lee, C. H. Fox, Z. Bao, *Nat. Nanotechnol.* **2011**, *6*, 788.

[33] T. Yamada, Y. Hayamizu, Y. Yamamoto, Y. Yomogida, A. Izadinajafabadi, D. N. Futaba, K. Hata, *Nat. Nanotechnol.* **2011**, *6*, 296.

[34] J. Narongthong, A. Das, H. H. Le, S. Wiessner, C. Sirisinha, *Compos. Pt. A-Appl. Sci. Manuf.* **2018**, *113*, 330.

[35] Y. J. Zheng, Y. L. Li, K. Dai, M. R. Liu, K. K. Zhou, G. Q. Zheng, C. T. Liu, C. Y. Shen, *Compos. Pt. A-Appl. Sci. Manuf.* **2017**, *101*, 41.

[36] D. Y. Wu, S. Meure, D. Solomon, *Prog. Polym. Sci.* **2008**, *33*, 479.

[37] X. Y. Cui, C. Zhang, R. P. Camilo, H. Zhang, A. Cobaj, M. D. Soucek, N. S. Zacharia, *Macromol. Mater. Eng.* **2018**, *303*, 8.

[38] R. P. Wool, *Soft Matter* **2008**, *4*, 400.

[39] M. D. Hager, P. Greil, C. Leyens, S. V. D. Zwaag, U. S. Schubert, *Adv. Mater.* **2010**, *22*, 5424.

[40] P. Cordier, F. Tournilhac, C. Souliéziakovic, L. Leibler, *Nature* **2008**, *451*, 977.

[41] L. Xing, Q. Li, G. Zhang, X. Zhang, F. Liu, L. Liu, Y. Huang, Q. Wang, *Adv. Funct. Mater.* **2016**, *26*, 3524.

[42] B. C. Tee, C. Wang, R. Allen, Z. Bao, *Nat. Nanotechnol.* **2012**, *7*, 825.

[43] G. B. Cai, M. Wada, I. Ohsawaa, S. Kitaoka, J. Takahashi, *Compos. Pt. A-Appl. Sci. Manuf.* **2018**, *107*, 555.

[44] X. Lu, T. Zhai, X. Zhang, Y. Shen, L. Yuan, B. Hu, L. Gong, J. Chen, Y. Gao, J. Zhou, *Adv. Mater.* **2012**, *24*, 938.

[45] D. Jiang, L. Xing, L. Liu, S. Sun, Q. Zhang, Z. Wu, X. Yan, J. Guo, Y. Huang, Z. Guo, *Compos. Sci. Technol.* **2015**, *117*, 168.

[46] D. Jiang, L. Liu, J. Long, L. Xing, Y. Huang, Z. Wu, X. Yan, Z. Guo, *Compos. Sci. Technol.* **2014**, *100*, 158.

[47] K. E. Korte, S. E. Skrabalak, Y. Xia, *J. Mater. Chem.* **2008**, *18*, 437.

[48] C. Wang, N. Liu, R. Allen, J. B. Tok, Y. Wu, F. Zhang, Y. Chen, Z. Bao, *Adv. Mater.* **2013**, *25*, 5785.

[49] R. Vaiyapuri, B. W. Greenland, H. M. Colquhoun, J. M. Elliott, W. Hayes, *Polym. Int.* **2014**, *63*, 933.

[50] D. Jiang, L. Xing, L. Liu, X. Yan, J. Guo, X. Zhang, Q. Zhang, Z. Wu, F. Zhao, Y. Huang, *J. Mater. Chem. A* **2014**, *2*, 18293.

[51] T. Yamada, Y. Hayamizu, Y. Yamamoto, Y. Yomogida, A. Izadinajafabadi, D. N. Futaba, K. Hata, *Nat. Nanotechnol.* **2011**, *6*, 296.

[52] Q. Fan, Z. Qin, S. Gao, Y. Wu, J. Pionteck, E. Mäder, M. Zhu, *Carbon* **2012**, *50*, 4085.

[53] B. Liang, Z. Lin, W. Chen, Z. He, J. Zhong, H. Zhu, Z. Tang, X. Gui, *Nanoscale* **2018**, *10*, 13599.